

Jan PEIRS\*, Patricia VERLEYSEN, Joris DEGRIECK  
Department of Mechanical Construction and Production, Ghent University (UGent)  
Sint-Pietersnieuwstraat 41, Ghent, Belgium

## THE USE OF HAT-SHAPED SPECIMENS FOR DYNAMIC SHEAR TESTING

*Received: 27 July 2008*

*Accepted: 27 August 2008*

In recent decades, specimens with hat-shaped geometry have been used to study materials with respect to their shear behavior including strain localization and adiabatic shear banding (ASB). However, the interpretation of the experimental results is still not straightforward because of the complex stress distribution in the shear region of the specimen. More comprehensive use of the hat-shaped specimen is possible when a better description of the distribution and evolution of the stress state in the specimen is available.

This paper presents the results of dynamic and static experiments on Ti-6Al-4V and numerical simulations in ABAQUS/Explicit. The stress, strain and temperature distribution and evolution is examined for specimens with varying dimensions. The aim is to identify the important factors that affect the experimental results.

Key words: experiment, simulation, hat-shaped specimen, Hopkinson

### 1. INTRODUCTION

In the past, a dozen of experimental techniques were developed to characterize the shear behavior and the process of the formation of adiabatic shear bands (ASB). A distinction should be made between techniques intended for the testing of bulk materials and sheet materials. This contribution focuses on one

---

\*Corresponding author. Tel.: +32 9 264 34 36; fax: +32 9 264 35 87  
E-mail address: [Jan.Peirs@UGent.be](mailto:Jan.Peirs@UGent.be) (J. Peirs)

frequently used technique for bulk materials which is based on the dynamic deformation of hat-shaped specimens in a split Hopkinson pressure bar (SHPB) setup.

Due to the specific geometry of the hat-shaped specimen, shear strains are concentrated in a narrow region where adiabatic shearing is likely to occur. This technique is particularly interesting for metallurgists because even materials that do not localize spontaneously in shear can be forced up to shearing failure. On the other hand, extracting material properties from these experiments is not straightforward because of the complex stress state in the shearing region.

More insight in the stress distribution in the specimen is needed in order to better understand the experimental data obtained by this technique. Furthermore, as the nucleation and propagation of ASBs depends on the stress condition [1], knowledge of the stress distribution is crucial. Moreover, several researchers used different specimen dimensions [2-7] in their experiments. The outcome of these experiments is affected not only by the tested material but also by the specimen geometry. This raises the question whether the results of different studies can be compared. Although, Bronkhorst [2] already investigated the stress distribution of one particular hat-shaped specimen geometry using FE simulations, different geometries have not been compared in detail.

The goal of this study was to relate the specimen dimensions with the stress and strain distribution and evolution in the specimen. This has previously been done for other specimen geometries: e.g. truncated-conic specimens [1], dog bone-shaped tensile specimens [8] and double shear specimens [9]. In addition, the existence of an optimal specimen geometry was studied to achieve a shearing stress state which is as pure as possible.

The main tool in this study is the FE method. Several slightly different geometries are simulated. The relation between geometry and global and local behavior of the specimen was studied. The stress and strain homogeneity was also examined. It can be concluded that the specimen geometry and small imperfections have a major influence on the experimental results. It was also found that the conditions of a homogeneous stress state and pure shear stress state cannot be accomplished together. Therefore, despite its simplicity, the technique with hat-shaped specimens seems to be of rather limited use.

A second purpose of these simulations was to find out whether it is possible or not to retrieve information about the shearing process (stress and strain) from the signals in the Hopkinson bars. The shear stress can be estimated quite easily but on the other hand the shear strain is impossible to determine. A post-mortem observation of the shear region is necessary to estimate the shear region width and the strain.

Hopkinson experiments and quasi-static experiments on a series of hat-shaped specimens of a Ti-6Al-4V alloy were carried out. The deformation in

some of these experiments was interrupted by means of a stopper ring. In this way, the material at an intermediate stage in the deformation process can be studied.

## 2. EXPERIMENTAL TECHNIQUE

The Hopkinson technique is ideally suited for dynamic experiments. The small specimen is placed between the two Hopkinson bars (Figure 1). Several specimen geometries are possible, depending on the type of the experiment. A loading wave  $\varepsilon_i$ , generated in the input bar, propagates along the bar towards the specimen. This wave interacts with the specimen and is subsequently partly reflected back into the input bar ( $\varepsilon_r$ ) and partly transmitted into the output bar. These three waves ( $\varepsilon_i$ ,  $\varepsilon_r$  and  $\varepsilon_t$ ) are measured by means of strain gages on the Hopkinson bars. From those waves, the total force and the global deformation of the specimen can be determined.

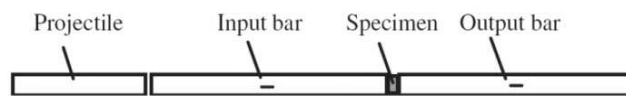


Figure 1: Sketch of a Hopkinson pressure bar set-up

In an axis-symmetric hat-shaped specimen, shear strains are concentrated in a narrow zone. Hence, even materials that do not localize spontaneously are forced to shearing failure by this method. Figure 2 shows the specimen between the two Hopkinson bars. The region where a shear band can develop has been marked.

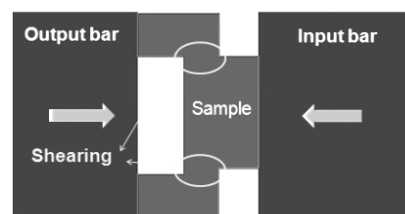


Figure 2: Principle of a Hopkinson test with hat-shaped specimen

Because all plastic deformation happens in the shearing region, the indentation of the hat can be estimated as the top-to-bottom surface displacement of the sample. This is classically done by integrating the velocity difference between the ends of the bars during the loading duration  $t$ :

$$\Delta u = 2C_b \int_0^t \varepsilon_r dt \quad (2.1)$$

with  $C_b$  - the wave speed in the bars. The obtained shear strain can be adjusted by choosing an appropriate hat indentation:  $\gamma = \frac{\text{indentation of the hat}}{\text{width of the localized region}}$ . The problem for a correct determination of  $\gamma$  is that the width of the localized region can only be estimated and is dependent on the material behavior. Therefore, post mortem analyses of the specimen are necessary.

The total load on the specimen can be determined from the transmitted wave by

$$P = A_b E_b \varepsilon_t \quad (2.2)$$

with  $A_b$  - the sectional area and  $E_b$  - the elasticity modulus of the Hopkinson bars.

Figure 3 shows a sketch of the specimen with an indication of characteristic lengths. Dimensions used in literature are given in Table 1. For most samples the inner radius  $r_1$  is slightly smaller than the outer radius  $r_2$  in order to have some normal pressure in the shear region.

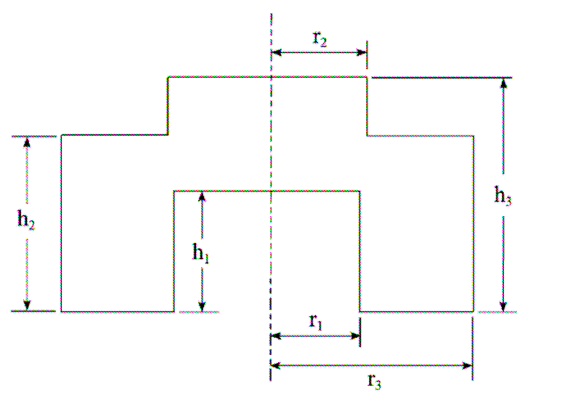


Figure 3: Specimen with indication of dimensions according to [2]

Hat-shaped specimens were used to study shear localization in tantalum and 316L stainless steel [2]. Tantalum was also studied by Nemat-Nasser [3]. Both researchers did the same kind of tests but, with different specimen geometry. The resulting stress-strain curves consequently did not match exactly. B.K. Kad studied a zirconium alloy [4] with this technique. Hat-shaped specimens were also used in studying 304L stainless steel [10] and 4340 high strength steel [5]. Couque [11] designed a modified geometry to study the formation of adiabatic shear bands in tungsten under a high hydrostatic pressure. Longère [12] used the same geometry for validation of the TEVPVD model (Thermo Elastic

ViscoPlastic with Viscous Deterioration). All the above mentioned investigators used other geometries so it's a logical question to ask how important the geometry is for the outcome of the experiments.

Table 1: Dimensions used in literature (all in mm)

Source	$r_1$	$r_2$	$r_1/r_2$	$r_3$	$h_1$	$h_2$	$h_2-h_1$	$h_3$
[2]	2.09	2.28	0.92	4.30	2.60	3.47	0.87	5.11
[3]	4.31	4.44	0.97	6.35	3.30	4.55	1.25	7.85
[4]	4.99	5.08	0.98	9.55	4.80	-	-	10.00
[5]	4.76	4.76	1	9.53	4.75	5.97	1.22	11.81
[6]	4.85	5.08	0.95	9.53	6.97	8.00	1.03	15.00
[7]	4	4.05	0.99	-	3.5	5.5	2	8.5
[13]	6.2	7.8	0.8	10	7	9.5	2.5	15.5

The main disadvantages of this testing method are the complex stress distribution in the specimen as well as the difficulty to observe the shear zone. The shear band will develop a subsurface. It is therefore impossible to track the shear band, detecting its temperature, measuring local strain, etc. Thus, this technique is appropriate for metallurgical research; shear bands can be made and investigated in a wide range of materials. On the other hand, the technique is less useful to study the mechanical properties of materials under dynamic loading. In order to overcome these disadvantages, more research on the influence of the specimen geometry on the formation of shear bands is useful.

The complex stress state in the shearing region is not always a disadvantage. For example, it appears that normal compressive stress and hydrostatic pressure can both retard shear fracture. But how these stresses affect the susceptibility of materials to adiabatic shear banding is unclear [14]. Altering the specimen geometry can give the possibility to experimentally study the influence of the stress state on the shear band formation. However, experimentalists can only take advantage of this plus point if the relation between specimen geometry and stress state is explicitly known. One aim of this study is to clarify the relation between characteristic lengths of the specimen and the resulting stress state.

### 3. EXPERIMENTAL RESULTS

#### 3.1. Material and method

Dynamic as well as quasi-static experiments were carried out. For the dynamic experiments a Hopkinson pressure bar setup with aluminum bars was

used while for the quasi-static experiments, an Instron 4505 test bench was used. Some dynamic experiments were interrupted at an intermediate stage of deformation by means of a stopper ring placed on the hat of the specimen. The displacement speed in the static experiments was 5mm/min.

The specimens were machined from an extruded Ti-6Al-4V bar ( $\varnothing$ 16mm). All tested specimens had slightly different dimensions (Table 2).

Table 2: Specimen dimensions (in mm), Exp4 is statically loaded while all other specimens were dynamically loaded

	<b>Exp1</b>	<b>Exp2</b>	<b>Exp3</b>	<b>Exp4</b>	<b>Exp5</b>
d1 (inner)	7.95	8.3	8	8.04	8
d2 (outer)	8.15	8.3	8.3	8.18	8.21
r1/r2	0.9755	1	0.9638	0.983	0.9744
h1	3.85	3.9	3.6	4	4.05
h2	5	5.1	4.9	5.02	5.05
h2-h1	1.15	1.2	1.3	1.02	1
h3	-	8.1	7.8	8	8.06
R	<	0.29	<	-	-
Stopper ring h	-	2.5	2.5	-	2.82

### 3.2. Results

The measured force-displacement curve of different experiments is shown in Figure 4. What all dynamic experiments have in common is a steep drop in the force after the force reaches a peak. This is due to the strain localization and subsequent adiabatic shear banding. The graph also shows that the results are highly scattered. This means that even small geometric differences of the specimens can have a clear effect on the results.

Figure 4 also includes a force-displacement curve of a quasi-static experiment (Exp4). In the static case, no global softening of the specimen is observed. Apparently, the deformation rate is too slow to cause a significant heating and thermal softening effect.

## 4. FE MODEL

Because the experimental results are not all consistent and because it's important to understand the experiment, in-depth, numerical simulations have been carried out. Therefore, a 2D axis-symmetric finite element model has been defined, using ABAQUS/Explicit. The load was applied by a uniform velocity ( $v=5000\text{mm/s}$ ) of the top-face of the specimen while the bottom-face was fixed.

The high displacement speed was achieved in  $20\mu\text{s}$  and the experiment lasted for  $100\mu\text{s}$ . Strain-rate and temperature dependency of the material behavior was modeled by the Johnson-Cook phenomenological model. Heat, generated by the plastic work, was included. Despite a short duration of the experiment, heat conduction was also included. Heat conduction seemed not important for the simulations of the dynamic experiments but it was important for the quasi-static experiments.

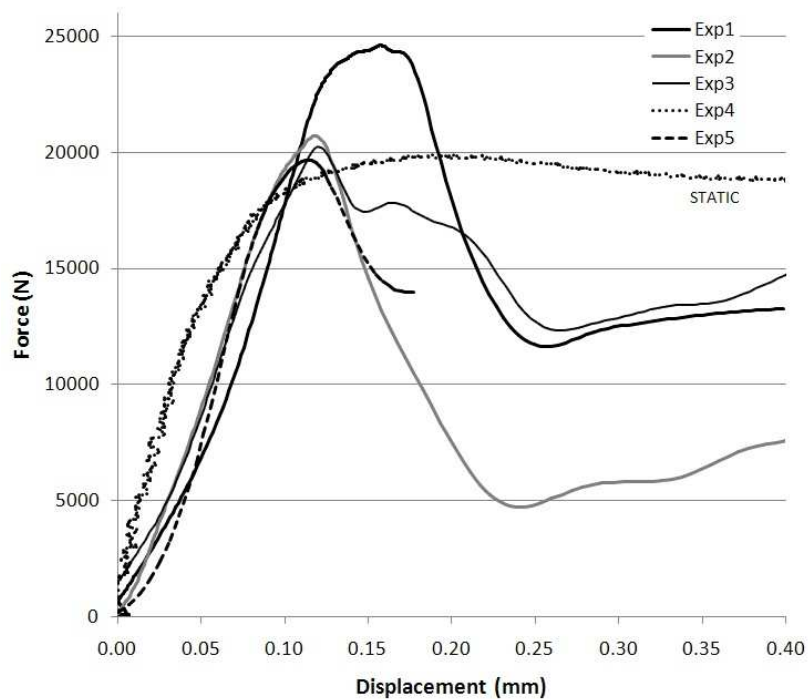


Figure 4: Force-Displacement curves of the experiments Exp1-Exp5; the static curve (Exp4) shows no drop in the force

The specimen was meshed with CAX4R elements; this is a 4-node bilinear axis-symmetric quadrilateral element with reduced integration. To obtain detailed information of the deformation and possible instability of the specimens, the dimensions of the elements within the shear band had to be less than the ASB width. Otherwise no ASB is expected due to the element-averaging effect [1]. For that reason, the mesh was strongly refined to  $15\mu\text{m}$  in the shearing region. To overcome difficulties caused by extensive element distortion, ALE adaptive meshing was used. In this way, a high quality mesh could be maintained without changing the number of elements.

Although the model was rate-dependent, mesh sensitivity of the simulations, after the strain was localized, could not be prevented. Moreover, since a phenomenological material model was used, the FE model was incapable of studying the shear band formation and propagation itself in detail. Nevertheless, the predicted global specimen response could provide good agreement with the experimental data.

The model is ideally suited to assess the stress, strain and temperature distribution and evolution in the specimen. The stress distribution in the shear region is illustrated for three time steps in Figure 5. Initially, two plastic regions were formed in the corners of the specimen. Those regions grew till the whole shear region was deforming plastically. Then, the deformation in the shear region was a combination of strain hardening and thermal softening. The strain localizes if the thermal softening effect overcomes the strain hardening effect. This causes a decreasing stress, first at the two corners and later along the whole shear region.

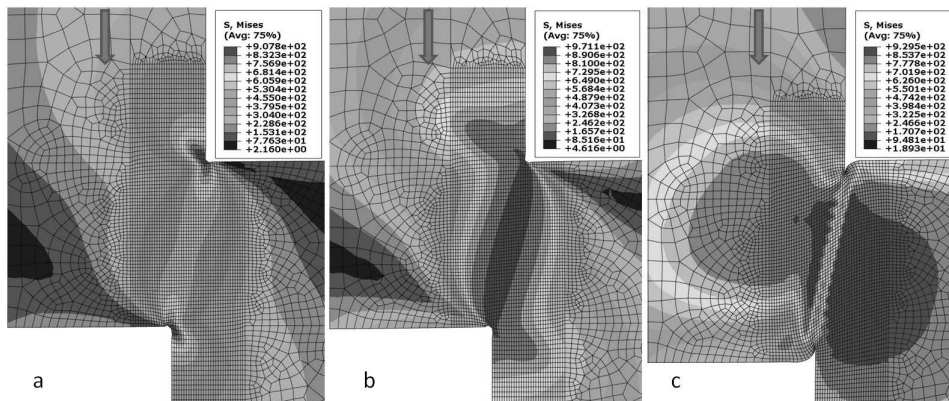


Figure 5: von Mises stress in the shear region of a hat-shaped specimen: a) 14 $\mu$ s, 0.03mm b) 20 $\mu$ s, 0.20mm c) 60 $\mu$ s, 0.25mm

## 5. THE EFFECT OF SPECIMEN GEOMETRY

Five series of simulations, each with a different dimension being varied, were performed. The goal was to relate some characteristic dimensions of the specimen to the occurring global response and stress state in the specimen. The following dimensions were varied: the width of the shear region characterized by  $r_1/r_2$ , the height of the shear region  $h_2-h_1$ , the radius of the corners  $R$ , the diameter  $r_3$  and the depth of the hole  $h_1$  (see Figure 6). The first three dimensions

seem to have a very important effect while the last two dimensions seem to have only a minor effect and will not be dealt with here.

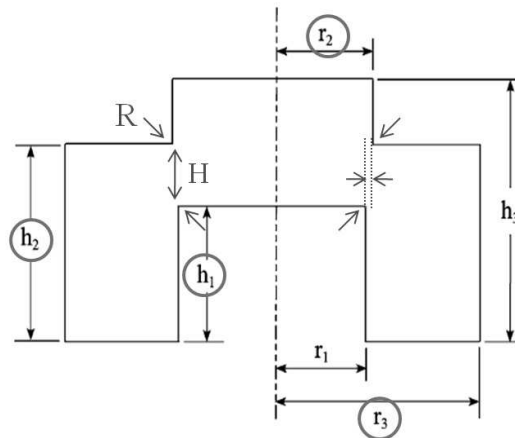


Figure 6: indication of the dimensions that were varied

### 5.1. Effect of the width of the shear region $r_1/r_2$

Six simulations with the  $r_1/r_2$  ratio varying from 1.05 to 0.9 are performed. The height of the shear region is 1mm for all specimens. The resulting force-displacement curve is shown in Figure 7. The simulated curves show the same trends as the obtained experimental curves: there is a steep drop in the force after a certain displacement.

As could be expected, the larger the shear region width (low  $r_1/r_2$ ), the higher the peak force needed to compress the specimen. The peak comes later for specimens with a large width of the shear region because for such specimen the strain is lower for the same displacement. From this, it's clear that the obtained force-displacement curve is very sensitive to this geometric characteristic.

In general, the stress state in the shear region is a combination of a deviatoric part (shear stress) and a hydrostatic part. A state of pure shear can never be achieved. The shear stress orientation is almost coincident with the geometric shear line (=connection between the two corners). The hydrostatic stress can be a tensile or a compressive stress, depending on the geometry and the moment in the deformation process. For specimens with  $r_1/r_2$  equal or slightly greater than 1, the stress state in the shear region is far from homogeneous. Some parts of the shear region are compressed while other parts are in a tensile stress state. Making the outer diameter of the specimen slightly bigger than the inner diameter ( $r_1/r_2 < 1$ ) causes the stress to become more homogeneous, which is better to have

a good experiment. On the other hand, if  $r_1/r_2$  becomes too low, it is more difficult to calculate the shear stress from the experimental results.

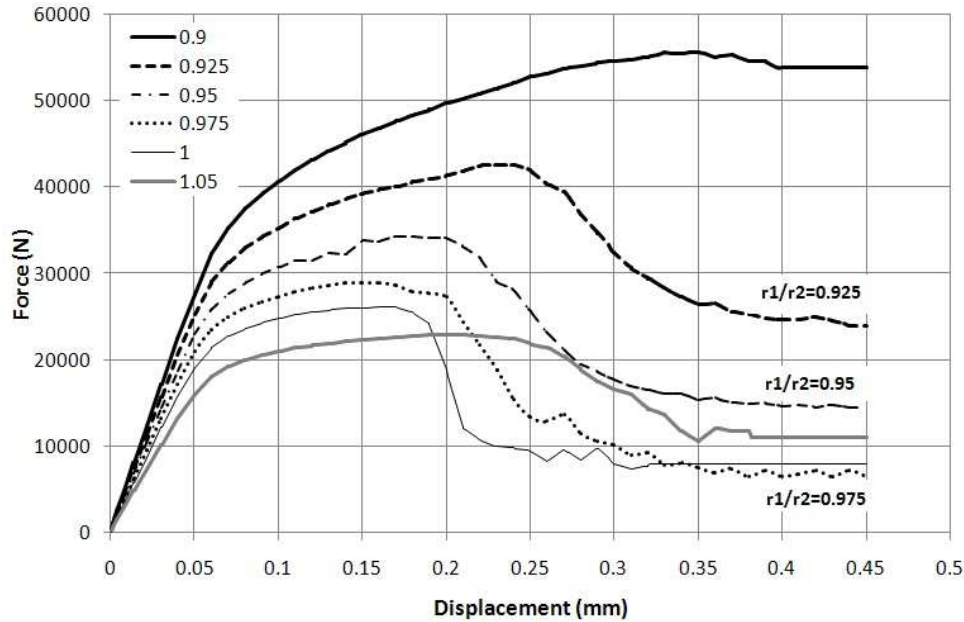


Figure 7: Force-Displacement curves: effect of the shear region width  $r_1/r_2$  and  $r_1=4\text{mm}$

With the signals recorded during a Hopkinson experiment, the total force on the specimen can be determined. However, the calculation of the shear stress from this force is not obvious. Therefore, the shear stress ratio (SSR) is defined:

$$\text{SSR} = \frac{\tau_{\text{centre}} \cdot A_{\text{SB}}}{F_V} \quad (5.1)$$

This value expresses the relation between the global vertical force on the specimen ( $F_V$ ) and the local stress in the center of the shear region ( $\tau_{\text{centre}}$ ).  $A_{\text{SB}}$  is the surface of the “shear band”.

Figure 8 shows the SSR for different specimen geometries as a function of the displacement. A constant SSR means that the measured force is in proportion with the shear stress in the shear region. If additionally the SSR is equal to 1, then the force is a good measurement of the shear stress. The interval where strain localization is expected to happen is shaded in gray.

Three different parts in all curves can be distinguished. In the beginning, the SSR is almost 0 for all specimens and increases rapidly. Indeed, the shear

stress is initially concentrated in the corners of the specimen. In the second part of the curve, the shear stress is homogeneous distributed along the shear region. This is approximately after a displacement of 0.05mm (20 $\mu$ s). Except for the low  $r_1/r_2$ -ratios, the SSR is quite constant in this interval. Finally, in the last part of the curves, the SSR decreases. This means that the force mainly contributes to the hydrostatic part of the pressure instead of to the shear stress component.

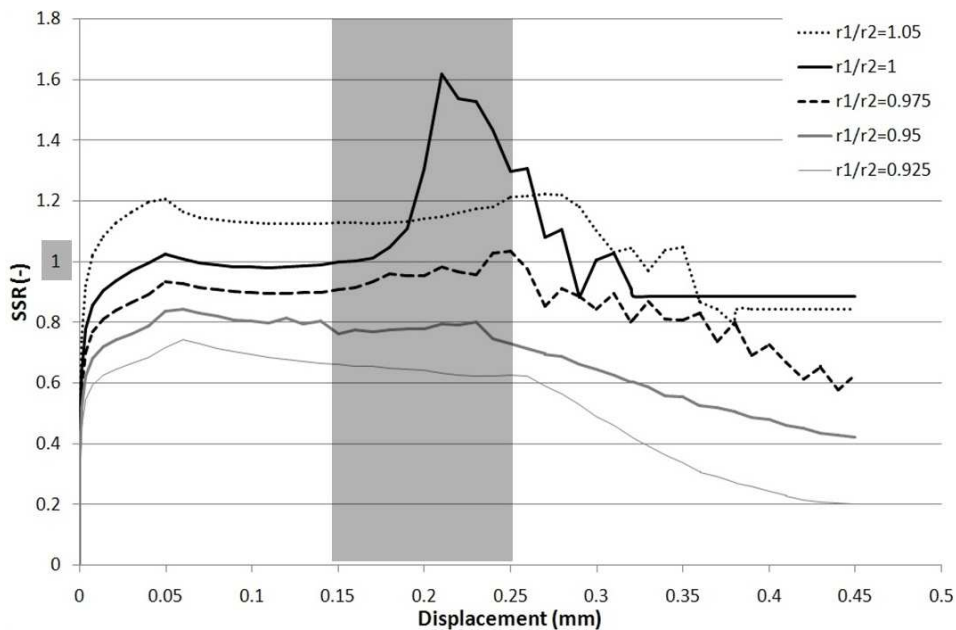


Figure 8: shear stress ratio as a function of the displacement for specimens with a different shear region width ( $r_1/r_2$ )

Three different parts in all curves can be distinguished. In the beginning, the SSR is almost 0 for all specimens and increases rapidly. Indeed, the shear stress is initially concentrated in the corners of the specimen. In the second part of the curve, the shear stress is homogeneous distributed along the shear region. This is approximately after a displacement of 0.05mm (20 $\mu$ s). Except for the low  $r_1/r_2$ -ratios, the SSR is quite constant in this interval. Finally, in the last part of the curves, the SSR decreases. This means that the force mainly contributes to the hydrostatic part of the pressure rather than to the shear stress component.

For a specimen with  $r_1/r_2=1$ , the SSR is initially very close to one but shows a peak at a displacement of 0.2mm. This means that the average shear stress in the shear region is much lower than the shear stress in the center of the specimen. So, inhomogeneous stress is the explanation for this peak in the SSR.

From this, it can be concluded that the specimen with  $r_1/r_2=0.975$  has the best performance: the force is a quite good measurement of the shear stress

(SSR almost 1) and the shear stress is quite homogeneous during the entire experiment.

### 5.2. Effect of the height of the shear region H

Three specimens with a different height of the shear region were simulated: 0.5mm, 1mm, 1.5mm. The width of the shear region was also adapted in order to have the same value of the angle of the geometric shear line (=line which connects the two corners). The force-displacement curves of these simulations are plotted in Figure 9.

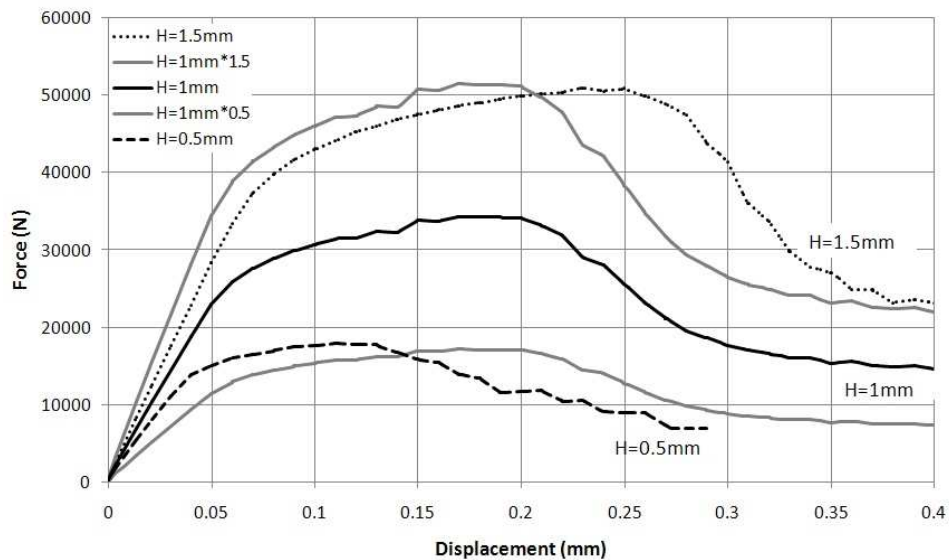


Figure 9: Force-Displacement curves: effect of the height of the shear region H; The gray curves represent the rescaled force of the specimen with H=1mm

Obviously, all the force-displacement curves have a similar course. The force from the specimen with H=1mm has been scaled up and down with a factor equal to the ratio of the shear heights. However, scaling only the force seems insufficient for the scaled curves to match with the force-displacement curves of the specimens with H=0.5 and H=1.5. There is also a scaling of the displacement: a higher displacement is necessary to achieve the same force. In other words, the strain is less concentrated for larger heights of the shear region.

### 5.3. Effect of the radius of the corners R

In the previously presented simulations, the corners of the specimen are sharp ( $90^\circ$ ). However, in actually machined specimens, the corners can be

rounded. Therefore, simulations were performed to see the effect of rounded rather than sharp corners.

In Figure 10 it can be seen that the effect of the radius  $R$  on the experimental results is huge. The total force is much higher for a specimen with rounded corners and the peak force is delayed. The rounded corners significantly reduce the stress concentration and therefore postpone strain localization. Stress concentrations are a trigger for shear localization to occur.

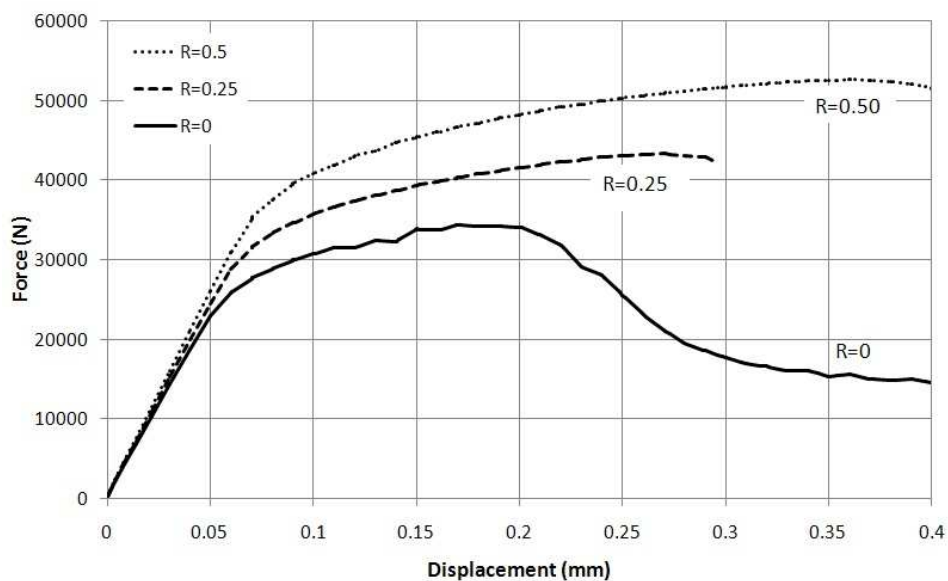


Figure 10: Force-displacement curves: effect of the radius of the corners

## 7. CONCLUSIONS

Both dynamic as well as quasi-static experiments with hat-shaped specimens were carried out. In order to better understand the experimental results, a numerical model in ABAQUS/Explicit was created. The model was used to find out the important factors that affect the outcome of the experiment.

The experimental results seem to be very sensitive to geometric variations. The influence of the width and height of the shear region and the radius of the corners is huge.

The second purpose of the model is to study the stress and strain distribution and evolution in the specimen. It is found that the conditions of a homoge-

neous stress state and pure shear stress state cannot be accomplished together for any investigated specimen geometry.

The shear stress ratio (SSR) is used to evaluate the relation between the total vertical force on the specimen and the shear stress in the center of the specimen. The shear stress in the center can only be obtained from the Hopkinson signals for specimens that have an outer diameter which is slightly larger than the inner diameter.

## 6. ACKNOWLEDGEMENTS

The authors would like to acknowledge The Interuniversity Attraction Poles Programme (IUAP) of the Federal Science Policy of Belgium and the partners of IUAP-VI ([www.m3phys.be](http://www.m3phys.be)).

## BIBLIOGRAPHY

- 1 Li JR., Yu JL., Wei ZG.: Influence of specimen geometry on adiabatic shear instability of tungsten heavy alloys, *International Journal of Impact Engineering*, 28 (2003) 303-314.
- 2 Bronkhorst CA., Cerreta EK., Xue Q., Maudlin PJ., Mason TA., Gray GT.: An experimental and numerical study of the localization behavior of tantalum and stainless steel, *International Journal of Plasticity*, 22 (2006) 1304-1335.
- 3 Nemat-Nasser S., Isaacs JB., Liu MQ.: Microstructure of high-strain, high-strain-rate deformed tantalum, *Acta Materialia*, 46 (1998) 1307-1325.
- 4 Kad BK., Gebert JM., Perez-Prado MT., Kassner ME., Meyers MK.: Ultrafine-grain-sized zirconium by dynamic deformation, *Acta Materialia*, 54 (2006) 4111-4127.
- 5 Beatty JH., Meyer LW., Meyers MA., Nemat-Nasser S.: Formation of controlled adiabatic shear bands in AISI 4340 high strength steel, *US-army materials technology laboratory* (1990).
- 6 Lins JFC., Sandim HRZ., Kestenbach H., Raabe D., Vecchio KS.: A microstructural investigation of adiabatic shear bands in an interstitial free steel, *Materials Science and Engineering a-Structural Materials Properties Microstructure and Processing*, 457 (2007) 205-218.
- 7 Lee WS., Liu CY., Chen TH.: Adiabatic shearing behavior of different steels under extreme high shear loading, *Journal of Nuclear Materials*, 374 (2008) 313-319.

- 8 Verleysen P., Degrieck J.: Experimental and numerical study of the response of steel sheet Hopkinson specimens, *Journal De Physique Iv*, 134 (2006) 541-546.
- 9 Klepaczko J.: Stress concentrators and rate effects in formation of adiabatic shear bands, European research office of the US-army (1996).
- 10 Meyers MA., Xu YB., Xue Q., Perez-Prado MT., McNelley TR.: Microstructural evolution in adiabatic shear localization in stainless steel, *Acta Materialia*, 51 (2003) 1307-1325.
- 11 Couque H.: A hydrodynamic hat specimen to investigate pressure and strain rate dependence on adiabatic shear band formation, *Journal De Physique Iv*, 110 (2003) 423-428.
- 12 Longere P., Dragon A., Trumel H., Deprince X.: Adiabatic shear banding-induced degradation in a thermo-elastic/viscoplastic material under dynamic loading, *International Journal of Impact Engineering*, 32 (2005) 285-320.
- 13 Teng X., Wierzbicki T., Couque H.: On the transition from adiabatic shear banding to fracture, *Mechanics of Materials*, 39 (2007) 107-125.
- 14 Bai Y., Dodd B.: *Adiabatic Shear Localization* (2de ed.), (1992) p. 379.